

Short Communication

## Study on the Properties of Jet Electrodeposited Nickel Coating by Rotating Interlacing Method

Lida Shen<sup>1,\*</sup>, Chuan Wang<sup>1</sup>, Zongjun Tian, Wei Jiang, Wei Zhuo, Kailin Zhao

College of Mechanical and Electrical Engineering, Nanjing University of Aeronautics and Astronautics, Yu Dao Street, 210016 Nanjing, China

\*E-mail: [ldshen@nuaa.edu.cn](mailto:ldshen@nuaa.edu.cn)

<sup>1</sup> These authors contributed equally to this work

Received: 1 October 2017 / Accepted: 24 November 2017 / Published: 28 December 2017

---

In order to improve the problem of inferior adhesion and poor protection performance of traditional coating on sintered NdFeB, a novel method involving discontinuous cathode rotation and interlaced deposition was proposed. For this study, the interlaced coating with thickness of 20  $\mu\text{m}$  was deposited on sintered NdFeB via interlaced jet deposition. The microstructures, surface morphologies were characterized using X-ray diffraction and scanning electron microscope, respectively. The adhesion strength was tested by automatic scratch tester. The corrosion behavior was analyzed by polarization curves. The results showed that the interlaced coating had fewer defects including cellular bulges, pits and pinholes, resulting in a uniform and smooth coating. The grain size decreased from 13.53nm of non-interlaced coating to 11.9nm. The adhesion strength increased significantly, from 17 N to 42 N. Compared with conventional nickel coating, multi-layer interlaced coating exhibited an enhanced corrosion resistance and can better protect NdFeB material.

---

**Keywords:** NdFeB permanent magnet; Jet electrodeposition; Interlacing; Adhesion strength; Corrosion resistance

### 1. INTRODUCTION

As a new energy material, sintered NdFeB magnet, with its excellent magnetic properties, has been widely used in wind power, aerospace, medical, industrial, electronics and other fields [1-5]. However, because of its multiphase microstructure, NdFeB is prone to oxidation in ambient and to the detrimental electrochemical corrosion under hot and humid atmospheres, which greatly limits its applications [6]. In order to improve its corrosion resistance, efficient protective coatings on the metal substrate surfaces are indispensable [7-16]. At present, the commonly used electrodeposition protective coatings are mainly as follows: Electrodepositing alloys such as Cu-Ni, Ni-Zn on NdFeB

substrate [7-9], electroplating Ni-P, Ni-Cu-Ni and Bright Ni-dark Ni multilayers coatings [10-13], electrodepositing composite coatings such as Ni-TiO<sub>2</sub> and Ni-Al<sub>2</sub>O<sub>3</sub> [14-16]. These researches have significantly improved the corrosion resistance of coatings, however, for alloy coatings, the standard reduction potential of different metals is quite apart and the metal content is difficult to control. For multilayers coatings, cross contamination between bath solutions is more likely to occur. For nanocomposite coating, nanoparticles are easy to aggregate. Those processes are relative complex and the above studies have little research on adhesion strength.

The corrosion resistance of the coating is closely related to adhesion strength between the substrate and the coating. Under poor adhesion strength, coating is easily affected by external impact, leading to damages such as blistering and peeling, thus, reducing the protective performance of the coating. At present, the primary techniques to improve the adhesion strength between NdFeB and the protective coating are by improving the pickling process [17, 18], pre-plating the base coat [19] and introducing ultrasonic assistance in electroless plating [20]. Both of these methods improve the adhesion strength effectively, but also significantly increase the complexity of the process.

Based on the characteristics of jet electrodeposition including low processing cost, large limiting current density and metal crystallization refinement, a novel method of discontinuous cathode rotation and interlaced deposition was presented in this study. Discontinuous cathode rotation served to change the surface state of the deposition surface below the nozzle and avoid continuous, preferential deposition in certain areas. Thus, the coating was able to grow homogeneously and compactly and coating defects are decreased. In addition, with the interlaced growth of the coating, increased interfaces blocked the continuous accumulation of the upper layer stress, and occlusal growth can further enhance the adhesion between substrate-layer as well as layer-layer, which can effectively improve the adhesion force. The proposed process is simpler than other technology.

## 2. EXPERIMENTAL

### 2.1 Experimental device

Fig. 1 shows the experimental device, which mainly includes three parts: the movement system, the fluid circulation system and the control system. Plating solution is pumped into the anode chamber and then injected onto the surface of the workpiece at high speed through nozzle. The anode chamber is filled with nickel beads to maintain the Ni<sup>2+</sup> content in the system. The movement system consists of three motors viz. the X axis motor drives the nozzle to traverse smoothly; Y axis motor drives the vertical movement of the anode, adjusting the machining gap; Z axis motor drives the rotation of the workpiece through a pair of bevel gears transmission. Thus the cathode rotation interlacing deposition is realized.

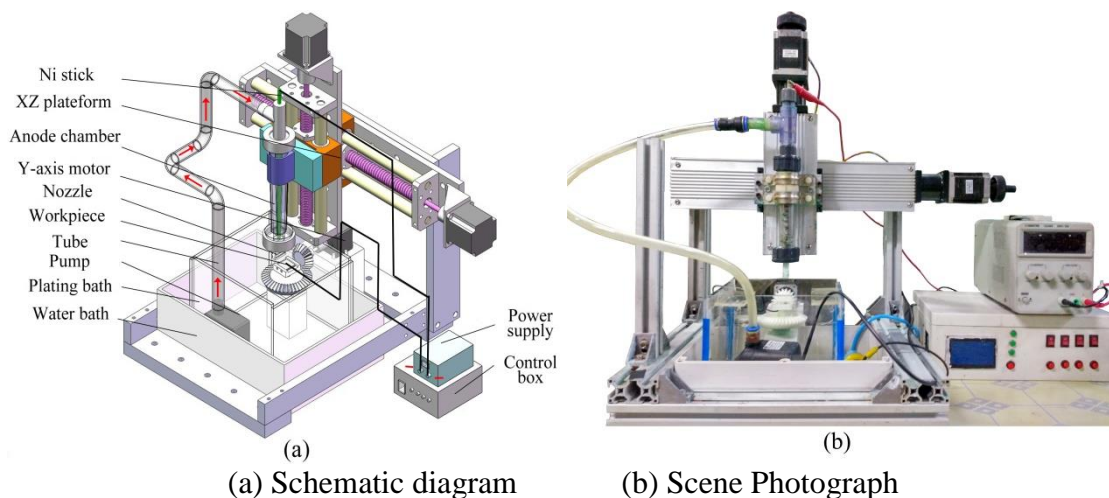


Figure 1. Experiment device

2.2 Cathode rotation device

In the process of jet electrodeposition, the cathode rotating device, as shown in Fig. 2, is designed in order to change the position of the workpiece in the plane, and realize the interlacing deposition of different angles. It mainly contains step motor, bevel gears, fixture and support. The Z axis motor drives the fixture together with the workpiece, rotating in the XZ plane through bevel gears transmission. Microstate of the substrate surface is random, which leads to the random influence of different interlacing angles on coating quality. Therefore, in order to facilitate the study, 90° is selected as the interlaced angle between layers. During the electrodeposition process, the nozzle moves back and forth along the X axis. After a certain time, the deposition system is turned off and the Z axis motor which drives the workpiece is rotated by 90°. Subsequently, the system power is turned on, completing the deposition on the other direction. This process is repeated until the desired thickness of the coating is achieved.

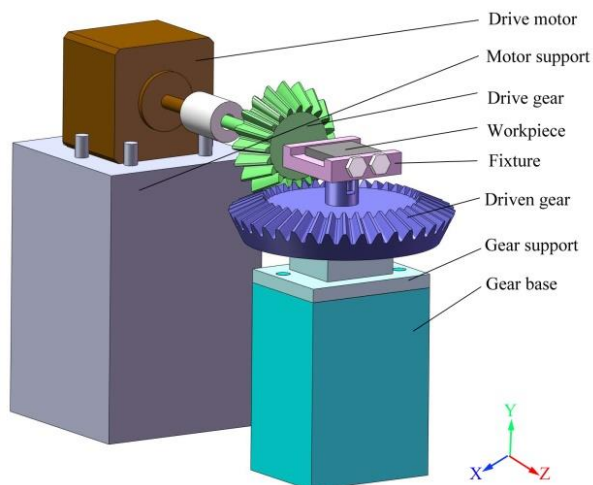


Figure 2. Rotating mechanism

### 2.3 Pretreatment

Sintered NdFeB specimens with a dimension of 30×30×3mm were used as substrates in this work. The composition is shown in Table 1. Before electrodeposition, the NdFeB magnet was first polished with an annular polishing machine to remove surface scratches. It was then rinsed with deionized water, ultrasonically degreased in alkaline solution, and was then sealed with zinc stearate. The prepared samples were subsequently polished by metallographic polishing machine with particle diameter of 3.5 μm diamond polishing agent until the mirror effect was achieved. Finally, the samples were cleaned with the deionized water and alcohol, and were dried and then reserved.

**Table 1.** NdFeB magnet composition

NdFeB	Nd	Fe	B	Ce	Al	Others
Wt%	23.08	68.67	0.99	5.23	1.02	1.01

### 2.4 Experiment content and parameters

In this paper, the one-time deposition of a certain orientation of the sample is considered as one layer. This experiment mainly studies the effect of different interlaced layers on coating performance. The coating thickness is approximately 20 μm. The sample number corresponding interlaced layers is shown in Table 2. The electrolyte composition and electrodepositing parameters in the experiment are shown in Table 3.

**Table 2.** Samples and the corresponding layers

Samples	1	2	3	4	5	6
Layers	1	7	15	31	63	127

**Table 3.** Bath compositions and operating conditions for Jet electrodeposition

Bath compositions and operating conditions	Quantity
NiSO <sub>4</sub> ·6H <sub>2</sub> O	280 g/L
NiCl <sub>2</sub> ·6H <sub>2</sub> O	40 g/L
H <sub>3</sub> BO <sub>4</sub>	40 g/L
C <sub>7</sub> H <sub>5</sub> O <sub>3</sub> NS	5 g/L
Temperature	50°C
Current density	100A/dm <sup>2</sup>
Time	20min

### 2.5 Test instrument

The surface morphologies of the coatings were investigated using a scanning electron microscope (SEM, model HITACHI-S4800). The microstructures were characterized by X-ray diffraction (XRD) spectrometer (D/max 2500VL/PC), operated at 40kV and 300mA with Cu-K $\alpha$  radiation ( $\lambda= 1.5406 \text{ \AA}$ ) to determine the phase composition and the crystallite size. The adhesion strength was tested by automatic scratch tester (model WS-2005, Zhongkekaihua Science and Technology Development Co., Lanzhou). The electrochemical experiments were performed in a three-electrode cell using a CHI-660E electrochemical working station in 3.5 wt% NaCl corrosive medium without agitation at the room temperature. The reference electrode was a saturated calomel electrode (SCE), and the counter electrode was a platinum electrode. The samples were immersed in the corrosive medium to attain open circuit potential ( $E_{ocp}$ ) about 30 min. Then the potentiodynamic sweeping was performed in the potential range of  $\pm 500 \text{ mV}$  with respect to the  $E_{ocp}$  by  $1 \text{ mV/s}$  sweeping rate. Electrochemical impedance spectra (EIS) were performed in an applied frequency ranged from  $10^5 \text{ Hz}$  down to  $10^{-2} \text{ Hz}$ .

## 3. RESULTS AND DISCUSSION

### 3.1 Surface morphologies

Fig. 3 shows the surface morphologies of traditional non-interlaced coating. As can be seen from Fig. 3a, there are many large cellular (cell-like) bulges on coating surface and even overlapping growth between adjacent bulges. Fig. 3b shows its corrosive surface morphologies after potentiodynamic polarization and electrochemical impedance spectra (EIS) examinations. It is clear that coating appeared larger corrosion pits in large cellular bulges, suffering severe corrosion, and some loose structures can be seen in corrosion pits. This is because, a large number of microscopic bulges inevitably exist on substrate surface. Meanwhile, the formation of the preferential crystal nucleus can also cause irregularities on cathode surface. Under relatively strong electric field, due to 'point discharge' effect, bulges have greater curvature, much denser equipotential surface, and the electric field strength is significantly enhanced [21], which results in the deposition velocity of micro bulges higher than that of smooth regions. As the deposition process continues, the electric field is shielded by large bulges, inhibiting the growth of the small bulges (as shown in Fig. 4). Subsequently, the growth of large bulges accelerates [22], eventually submerging the small bulges, then loose structures are formed between large bulges, which seriously deteriorates the density and uniformity of the coating. As a result, coating is prone to corrosion as shown in Fig. 3b. Thus, it is particularly important to reduce cellular bulges and improve the uniformity and compactness of coating. The scanning electrodeposition schematic diagram of conventional jet electrodeposition is shown as Fig. 5a.

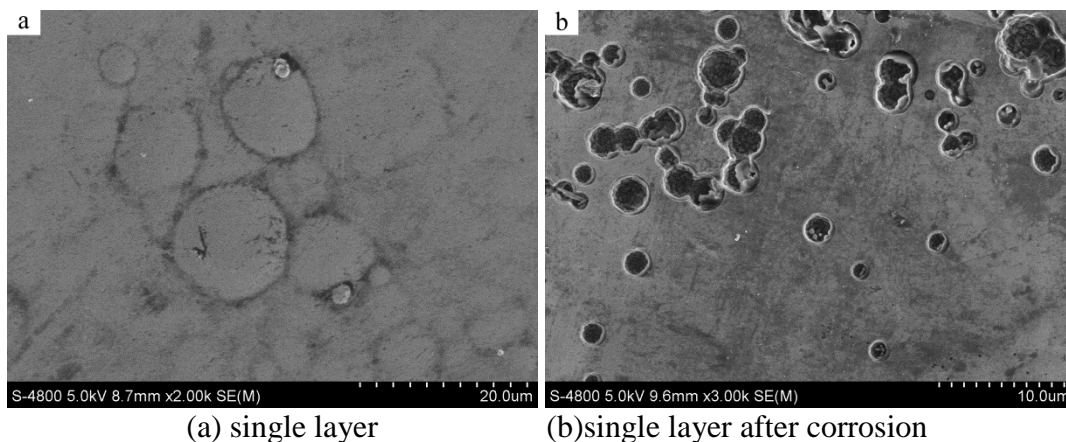


**Figure 3.** Surface morphology of nickel coatings

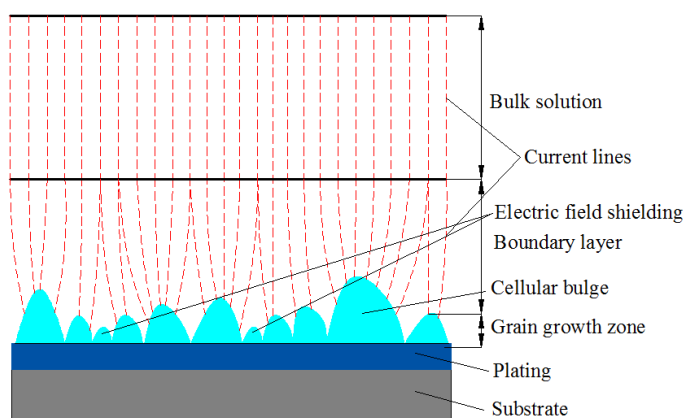


**Figure 4.** Cellular bulges' effect on current lines

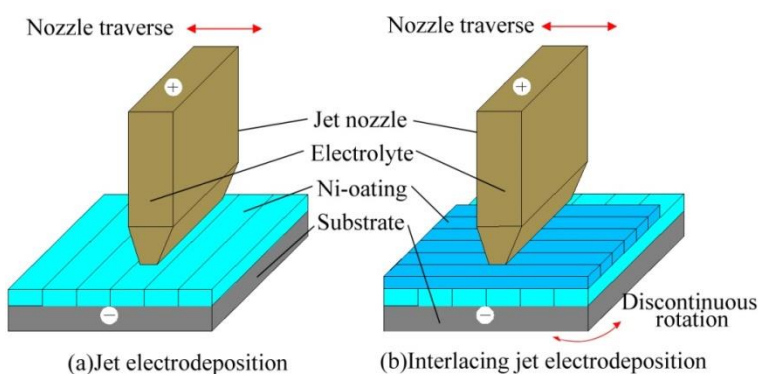


**Figure 5.** Electrodeposition schematic diagram

Interlacing jet electrodeposition schematic diagram is shown as Fig. 5b. Fig. 6 shows the surface morphologies of interlaced coatings with different layer. With the introduction of interlaced deposition, the size and amount of cellular bulges evidently decreased and 63 layer-coating (Fig. 6d) had the best surface quality. As shown in Fig. 6e, when interlaced layer number increased to 127 layers, i.e. when the thickness of the monolayer was about 0.16  $\mu\text{m}$ , despite the surface bulges of the

coating was greatly improved, because of frequent interlacing, short single-layer deposition time as well as the restriction of experimental device and process, the complete and compact monolayer film was difficult to be plated, which resulted in a few pits, pinholes and other defects on the surface. Fig. 6f shows the corrosive surface of interlaced 63 layer-coating. Compared with Fig. 3b, coating surface remained smooth, the size of corrosion pins decreased significantly. This is because, for interlaced jet electrodeposition, when the workpiece rotated at a certain angle, the electric field distribution on the surface under the nozzle changed. The growing points, shielded in last layer have a great chance of breaking through the shield, and re-growing. Interlacing reduced uneven growth time influenced by ‘point discharge’ effect. It also reduced ‘shielding effect’, causing the growth capacity of growing points on the whole deposition surface was fully developed, making the deposition more uniform and compact.

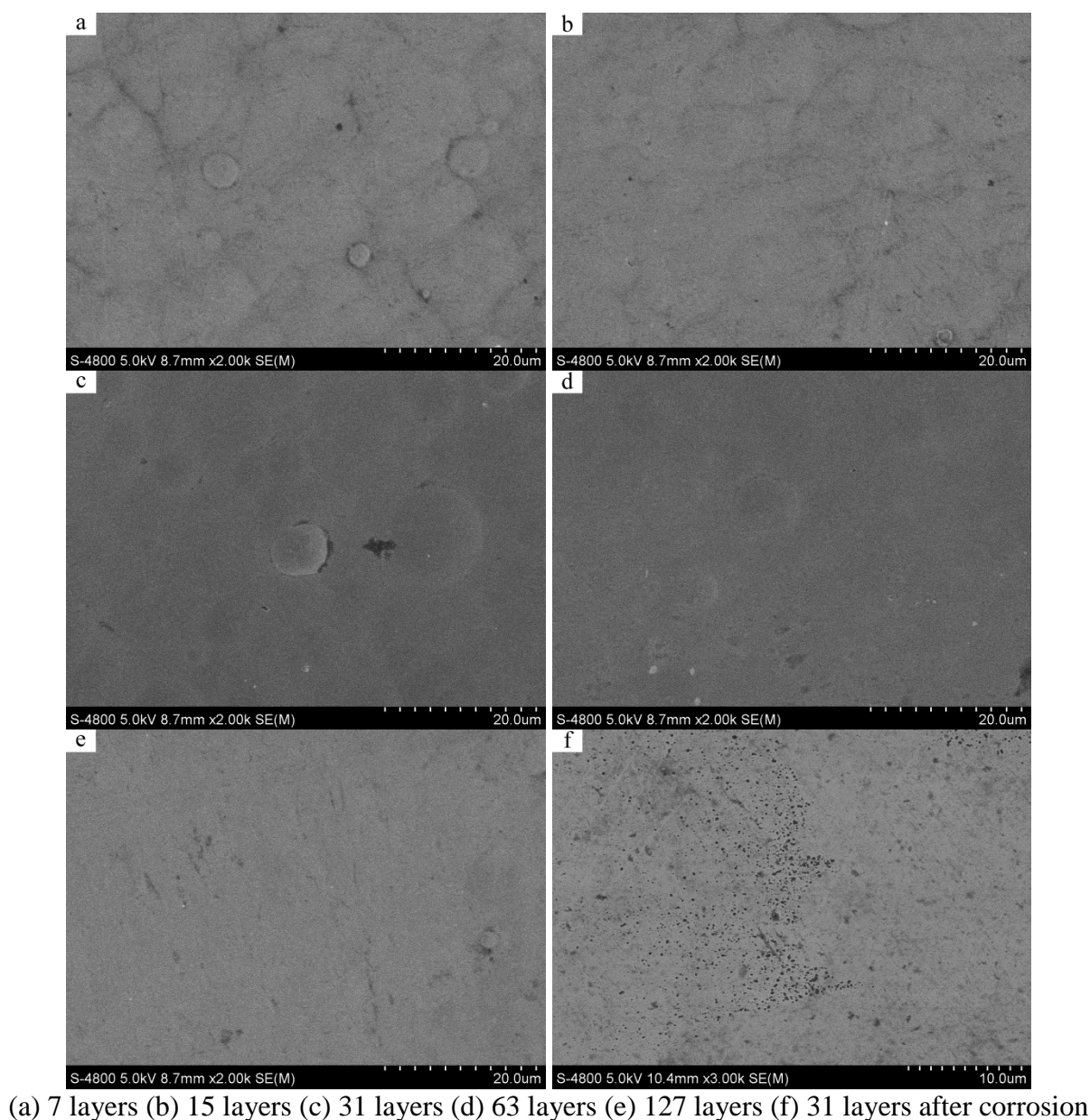
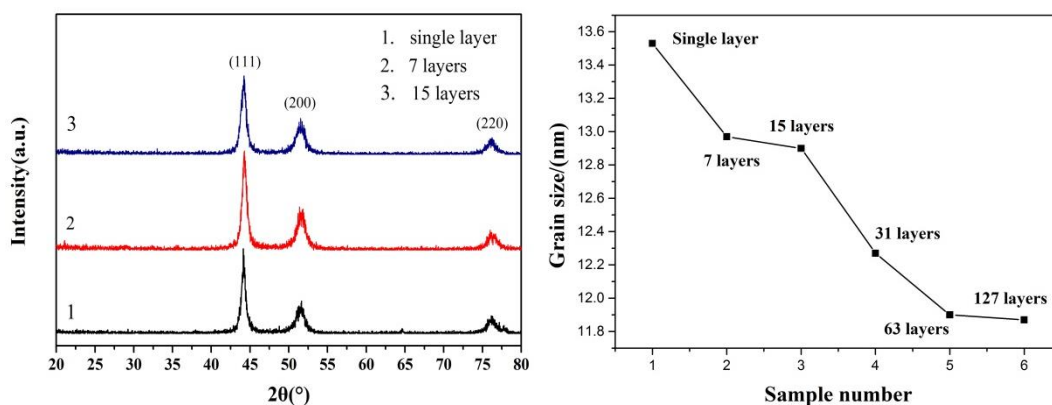


Figure 6. Surface morphology of interlaced nickel coatings

### 3.2 Microstructure

Fig. 7a shows the X-Ray Diffraction patterns of single layer and interlaced coatings. A comparison with the Ni standard map shows that the structure was face-centered cubic structure, the corresponding crystal plane of the diffraction peak of the coating were (111), (200), and (220). As can be seen from the figure, under this process condition, the introduction of interlacing had little effect on crystal plane growth of the coating, the growth of Ni coatings was still dominated by the (111) crystal plane. The grain size calculated for each coating is shown in Fig. 7b. The non-interlaced single-layer film had the largest grain size, which was 13.53 nm. With the increasing of interlaced layers, the grain size exhibited refinement. The grain size of 63 layers was about 11.9 nm. Jun Zhu [23] reduced the grain size of Ni coating from 15nm to 10nm by means of friction assisted jet electrodeposition. The reason is that mechanical friction can help break crystals when they grow too fast, leading to the formation of many new screw dislocation outcrops, which facilitate crystal nucleation, increase the rate of nucleation, and refine the grain eventually.

Cathode rotating interlaced jet electrodeposition can fully exploit the growth ability of each growing points, improve point discharge and shielding effects of large cellular bulges, so that the entire deposition surface grows uniformly, rather than the preferential growth of some nucleation points. That is, in contrast to traditional jet electrodeposition, interlaced jet electrodeposition provides more nucleation points for coating deposition. In addition, the interlaced growth of coating can effectively restrain the growth of columnar structure of single layer metal and limit the growth of the grain, resulting in a refined grain.



**Figure 7.** (a) XRD patterns of Ni coating (b) Coating grain size of different layers

### 3.3 Adhesion strength

The cross-section morphology of nickel coating on NdFeB magnets is shown in Fig. 8. Fig. 8a shows that there was slight gap between coating and substrate, the combination was not ideal, while the adhesion of the interlaced 63 layers in Fig. 8b was very tight. Fig. 9 shows the adhesion strength measured by automatic scratch tester. As shown in Fig. 9a, the friction curve had a large fluctuation around 17 N, so the adhesion strength of non-interlaced layer was 17 N. Similarly the adhesion

strength of interlaced 63 layers was 42 N. The adhesion strength force test results were consistent with the actual cross-section morphology. The adhesion strength of different interlaced layers is shown in Fig. 10. With the increase of the number of interlacing layers, the adhesion strength showed a clear improvement. For 63 layers, the adhesion strength reached the maximum value of 42 N. However, upon further increased in number of layers to 127 layers, the adhesion strength decreased sharply.

Ni coating is known to be high stress coating. With the increase of coating thickness, the coating tensile stress was accumulated gradually [24], which led to a tendency of breaking away from the substrate, as shown in Fig. 8a. For traditional jet electrodeposition, the shape and size of the once-forming coating were similar to the outlet section of the nozzle, to form the complete coating of the entire deposition surface the nozzle was required to traverse. The structure and stress difference of the once forming coating were small, while the stress difference of the coating deposited by reciprocating scanning was large [25]. As the stress of coating was an important factor affecting the adhesion strength, so for conventional jet electrodeposition, when testing in parallel or perpendicular to the scanning direction by coating scratch tester, the results were often very different, the test results perpendicular to the scanning direction were greater than parallel to the scanning direction, which greatly limited the adhesion performance of the coating in practice. As it can be observed from Fig. 9, the fluctuation of friction curves of interlaced coating was smaller than that of single layer, indicating that after the introduction of interlacing, with the frequent rotation of the cathode workpiece and the continuous interlaced deposition in different directions, the difference between the above mentioned two directions of coating gradually decreased, thus the internal stress of the coating tended to be uniform. For one hand, the thickness of monolayer film decreased, with the interlaced growth of the coating, increased interfaces blocked the continuous accumulation of the upper layer stress, and thus the inherent stress was alleviated. The tendency of coating break away from the substrate was also reduced. For another hand, the 'netted' occlusal growth between interlaced layers further strengthened the adhesion strength. Therefore, the interlaced coating exhibited a clearly increased adhesion. However, when interlacing was too often, single-layer deposition time was too short to deposit complete monolayer film. In addition, during the interlacing rotation and transposition process, the incomplete monolayer film was continuous injected by high-speed spraying liquid, which further affected the occlusal growth of coating. Therefore, the adhesion strength decreased.

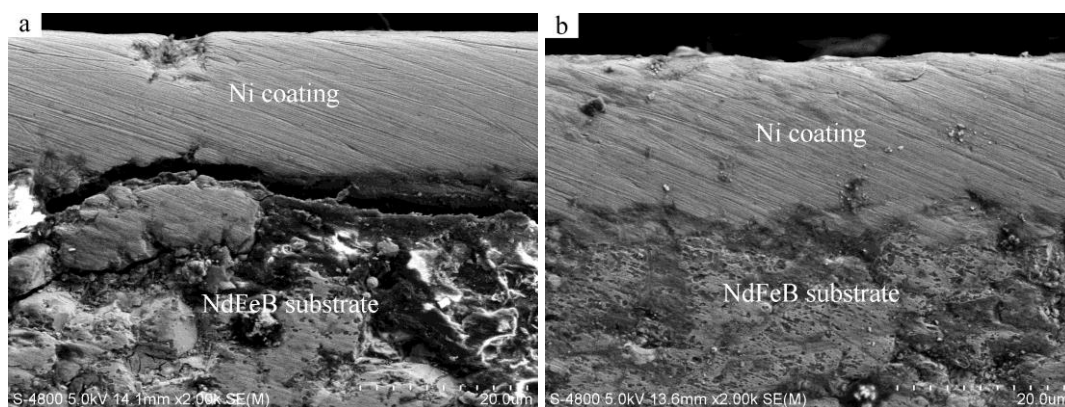


**Figure 8.** Cross-section morphologies of Ni coating on Sintered NdFeB (a) Single layer (b) 63 layers

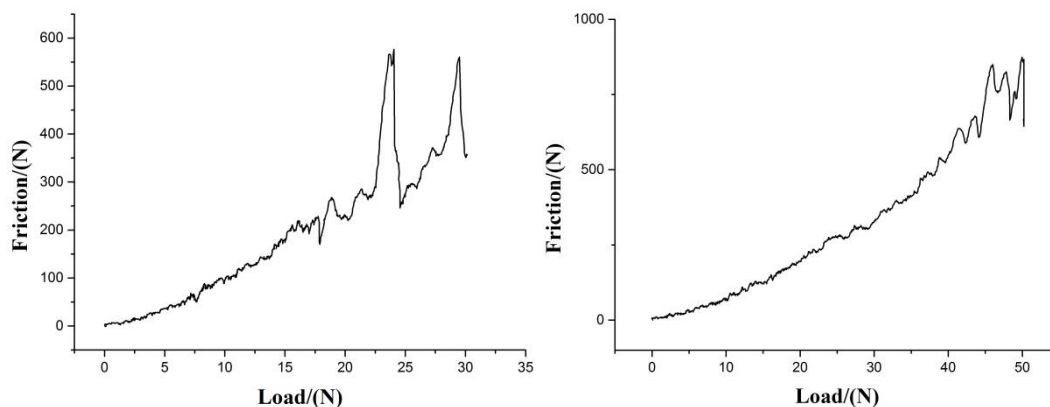


Figure 9. Adhesion strength test curves measured by scratch tester (a) Single layer (b) 63 layers

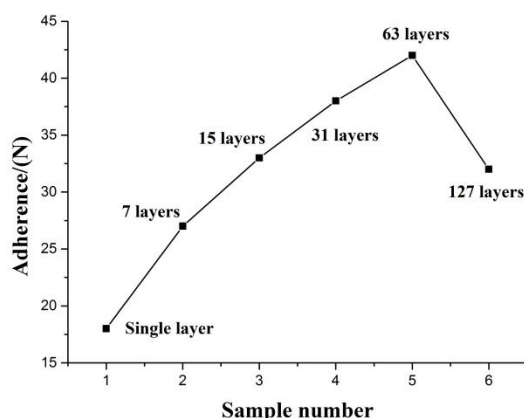


Figure 10. Adhesion strength of Ni coating on Sintered NdFeB with different layers

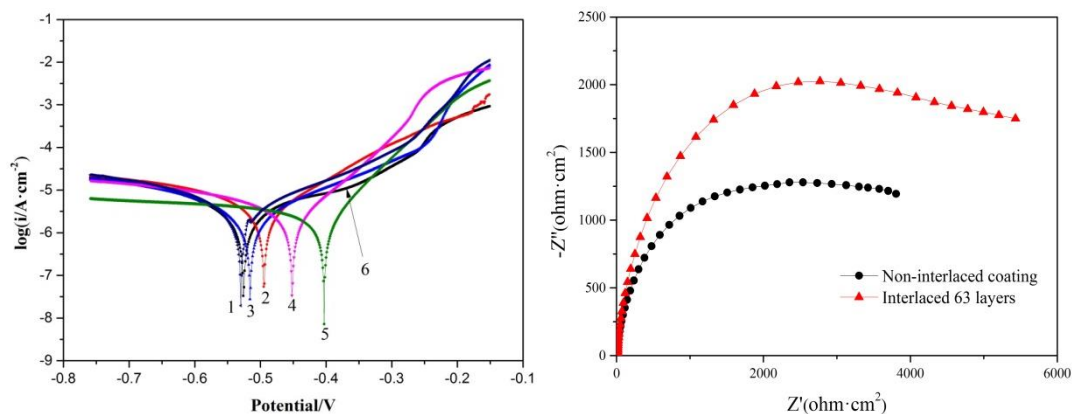
### 3.4 Corrosion resistance

Fig. 11a shows the potentiodynamic polarization curves of different interlaced layers Ni coatings in 3.5 wt% NaCl solution. The corrosion potential  $E_{corr}$  and current density  $I_{corr}$  calculated by Tafel extrapolation are listed in Table 5.

As can be seen from Table 5, compared with non-interlaced coating, the corrosion current density of the interlaced coating decreased and the corrosion potential moved towards positive direction, indicating an improved corrosion resistance. With the increase of the number of interlaced layers, the corrosion current density decreased and the corrosion potential continued to move forward. When the number of layers was 63, the corrosion current density dropped from 4.98 to 2.09  $\mu\text{A}\cdot\text{cm}^{-2}$  and the corrosion potential moved from -0.530V to -0.403 V. So, interlaced 63 layers not only showed lower corrosion tendency but also displayed lower corrosion speed in the event of an onset of corrosion. When the number of interlaced layers increased to 127, the corrosion resistance notably decreased. Electrochemical impedance spectra of non-interlaced coating and interlaced 63 layers coating were obtained and shown as Nyquist plots in Fig. 11b, it is obvious that the capacitive loop radius of interlaced 63 layers coating was larger than that of non-interlaced coating, indicating higher polarization resistance, i.e., stronger corrosion resistance. Wei Zhuo [22] improved corrosion

resistance of Ni coating by introducing friction assistance, the corrosion current density is reduced from 3.984 to 1.009  $\mu\text{A}\cdot\text{cm}^{-2}$ . Yihao Wang [26] improved corrosion resistance of Ni coating by adding  $\text{SiO}_2$  nanoparticle, the corrosion current density is reduced from 3.583 to 1.354  $\mu\text{A}\cdot\text{cm}^{-2}$ . Compared with those studies, interlacing jet electrodeposition can also improve coating corrosion resistance, and the technology is much easier.

Material corrosion originates from surface, especially defect. For conventional jet electrodeposition, due to point discharge and shielding effects, it is easy for coatings to produce cellular bulges and continue to deposit, the growth of the large bulges accelerate, eventually submerging small bulges, which seriously deteriorates coating density and uniformity. The generated loose structures provide routes for corrosive ions to permeate. As a result, coating is prone to corrosion as shown in Fig. 3b. Interlaced jet electrodeposition can improve this shield effect and give full play to the growth ability of growing points on the whole deposition surface, so that the coating is more uniform and compact. This makes it difficult for corrosive ions to permeate into coating. In addition, layer-layer alternative deposition can relax stress and reduce the occurrence of micro cracks, which usually provide channels for the transport of corrosion ions. What is more, the increased interfaces further blocked the permeation of corrosive ions. Therefore, the corrosion resistance of interlaced coatings improved.



**Figure 11.** (a) Potentiodynamic polarization curves and (b) Nyquist plots of Ni coating on NdFeB in 3.5 wt% NaCl solution.

**Table 5.** Electrochemical data of different interlaced layers of Ni coated on NdFeB.

Samples	Interlaced layers	$E_{\text{corr}}/\text{V}$	$i_{\text{corr}}/\mu\text{A}\cdot\text{cm}^{-2}$
1	1	-0.530	4.98
2	7	-0.495	3.82
3	15	-0.516	2.88
4	31	-0.452	2.50
5	63	-0.403	2.09
6	127	-0.526	4.02

However, when the number of interlaced layers is too many, single-layer deposition time is too short to deposit complete monolayer film. In addition, during the interlaced rotation and transposition process, the incomplete monolayer film was continuously injected by high-speed spraying liquid, which further affected the occlusal growth of coating. Thus there are more micro pores in each monolayer, which provides channels for corrosion ions, so the corrosion resistance will be reduced again.

#### 4. CONCLUSIONS

(1) Compared with conventional jet electrodeposition, the discontinuous cathode rotating interlaced deposition has the advantage of improving point discharge and shield effects, so it can reduce cellular bulges and make coatings more uniform and compact, thus improve coatings quality.

(2) Interlaced deposition can refine grain size, from 13.53 to 11.9 nm under the experimental conditions in this study.

(3) The introduction of interlacing can improve adhesion strength. With the increase of the number of layers (the thickness of monolayer decreases), the improvement is more obvious, from 17 N to 42N (63 layers). However, when the number of layers is too many, the occlusal growth is affected, so the resulting adhesion strength decreases.

(4) Interlaced jet electrodeposition can effectively improve the uniformity and compactness of coatings, reduce the defects of the coating and improve the corrosion resistance.

#### ACKNOWLEDGEMENT

The project is supported by the National Natural Science Foundation of China (grant No. 51475235 and No. 51105204). We also extend our sincere thanks to all who contributed in the preparation of these instructions.

#### References

1. Y. Matsuura, *J. Magn. Magn. Mater.*, 303 (2006) 344.
2. O. Gutfleisch, M.A. Willard and E. Bruck, *Adv. Mater.*, 23 (2011) 821.
3. T.Q. Zhang, F.G. Chen and Y. Zheng, *Intermetallics*, 73 (2016) 67.
4. B. Ma, A.Z. Sun and Z.W. Lu, *J. Magn. Magn. Mater.*, 416 (2016) 150.
5. A.G. Popov, V.S. Gaviko and N.N. Shchegoleva, *J. Magn. Magn. Mater.*, 386 (2015) 134.
6. L.A. Dobrzanski, M. Drak and J. Trzaska, *J. Mater. Process Tech.*, 164 (2005) 795.
7. L. Zhang, C. Jing, *Electron. Process Tech.*, 30 (2009) 230.
8. M. Alper, H. Kockar and M. Safak, *J. Alloys Compd.*, 453 (2008) 15.
9. E. Pellicer, A. Varea and S. Pané, *Adv. Funct. Mater.*, 20 (2010) 983.
10. Z. Chen, A. Ng and J.Z. Yi, *J. Magn. Magn. Mater.*, 302 (2006) 216.
11. I. Rampin, F. Bisaglia and M. Dabalà, *J. Mater. Eng. Perform.*, 19 (2010) 970.
12. C.B. Ma, F.H. Cao and Z. Zhang, *Appl. Surf. Sci.*, 253 (2006) 2251.
13. L.D. Shen, Y.H. Wang and W. Jiang, *Corros. Eng., Sci. Technol.*, 52 (2017) 311.
14. Q. Li, X.K. Yang and L. Zhang, *J. Alloys Compd.*, 482 (2009) 339.
15. H. Zhang, Y.W. Song and Z.L. Song, *Mater. Corros.*, 59 (2008) 324.
16. X.K. Yang, Q. Li and S.Y. Zhang, *Mater. Corros.*, 61 (2010) 618.
17. X.H. Cheng, J. Li and X.J. Yu, *Met. Funct. Mater.*, 20 (2013) 24.

18. Q.Y. Zhou, G. Li and Z. Liu, *J. Rare Earth.*, 34 (2016) 152.
19. W. Liu, J. Hou, *Plating and Finishing*, 34 (2012) 20.
20. M. Yan, H.G. Ying and T.Y. Ma, *Mater. Chem. Phys.*, 113 (2009) 764.
21. X. Liu, L.D. Shen and M.B. Qiu, *Surf. Coat. Technol.*, 305 (2016) 231.
22. W. Zhuo, L.D. Shen, M.B. Qiu, Z.J. Tian and W. Jiang, *Surf. Coat. Technol.*, 333 (2018) 87.
23. J. Zhu, Z.J. Tian, Z.D. Liu, L.D. Shen, Y.H. Huang and G.F. Wang, *J. South China Univ. Technol. Nat. Sci. Ed.*, 39 (2011) 92.
24. Z.W. Xie, J. Zhu and W. Guo, *Mater. Charact.*, 44 (2000) 347.
25. C. Xu, L.D. Shen, Z.J. Tian, Z.D. Liu, Y. Ma and J. Zhu, *Mater. Mech. Eng.*, 39 (2015) 35.
26. Y.H. Wang, L.D. Shen, M.B. Qiu, Z.J. Tian, X. Liu and W. Zhuo, *J. Electrochem. Soc.*, 163 (2016) 579.

© 2018 The Authors. Published by ESG ([www.electrochemsci.org](http://www.electrochemsci.org)). This article is an open access article distributed under the terms and conditions of the Creative Commons Attribution license (<http://creativecommons.org/licenses/by/4.0/>).